

Article

On the Dehydrocoupling of Alkenylacetylenes Mediated by Various Samarocene Complexes: A Charming Story of Metal Cooperativity Revealing a Novel Dual Metal σ -Bond Metathesis Type of Mechanism (DM| σ -BM)

Christos E. Kefalidis * and Laurent Maron *

CNRS (Centre National de la Recherche Scientifique) & INSA (Institut National des Sciences Appliquées), UPS (Université Paul Sabatier), LPCNO (Laboratoire de Physique et Chimie des Nano-objets), Université de Toulouse, 135 Avenue de Rangueil, Toulouse F-31077, France

* Authors to whom correspondence should be addressed; E-Mails: christos.kefalidis@gmail.com (C.E.K.); laurent.maron@irsamc.ups-tlse.fr (L.M.); Tel.: +33-561-559-664 (C.E.K. & L.M.).

Academic Editors: Stephen Mansell and Steve Liddle

Received: 30 September 2015 / Accepted: 26 November 2015 / Published: 4 December 2015

Abstract: The prevailing reductive chemistry of Sm(II) has been accessed and explored mostly by the use of samarocene precursors. The highly reducing character of these congeners, along with their Lewis acidity and predominantly ionic bonding, allows for the relatively facile activation of C–H bonds, as well as peculiar transformations of unsaturated substrates (e.g., C–C couplings). Among other important C–C coupling reactions, the reaction of phenylacetylene with different mono- or bimetallic samarocene complexes affords trienediyl complexes of the type $\{[(C_5Me_5)_2Sm]_2(\mu-\eta^2:\eta^2-PhC_4Ph)\}$. In contrast, when *t*-butylacetylene is used, uncoupled monomers of the type $(C_5Me_5)_2Sm(C\equiv C-tBu)$ were obtained. Although this type of reactivity may appear to be simple, the mechanism underlying these transformations is complex. This conclusion is drawn from the density functional theory (DFT) mechanistic studies presented herein. The operating mechanistic paths consist of: (i) the oxidation of each samarium center and the concomitant double reduction of the alkyne to afford a binuclear intermediate; (ii) the C–H scission of the acetylinic bond that lies in between the two metals; (iii) a dual metal σ -bond metathesis (DM| σ -SBM) process that releases H₂; and eventually (iv) the C–C coupling of the two bridged μ -alkynides to give the final bimetallic trienediyl complexes. For the latter mechanistic route, the experimentally used phenylacetylene was considered first as well as the aliphatic hex-1-yne. More interestingly, we shed light into the formation of

the mono(alkynide) complex, being the final experimental product of the reaction with *t*-butylacetylene.

Keywords: samarium; σ -bond metathesis; trienediyl; C–C coupling; mechanism; DFT calculations; bimetallic complexes; terminal alkynes

1. Introduction

The versatility of coupling reactions mediated by single-electron transfer (SET) from Sm(II) complexes is clearly illustrated by the chemistry of SmI₂ [1,2]. This coupling chemistry has been expanded by the use of (Cp*)₂Sm(THF)_{*n*} (where Cp* = C₅Me₅; *n* = 0–2) [3–7]. Interestingly, both the Lewis acidity and the ionic bonding of these Sm(II) complexes offer ligation of substrates that can undergo facile activation of C–H bonds, or partial reduction of unsaturated compounds [8]. These two elementary steps can combine to achieve dehydrocoupling of alkynes, as was initially reported by Evans in the case of phenylacetylene. This led to the characterization of a new class of dinuclear Sm(III) trienediyl complexes, {[(Cp*)₂Sm]₂(μ - η^2 : η^2 -PhC₄Ph)} [9]. These trienediyl species were obtained by four different reaction procedures: (a) the reaction of (Cp*)₂Sm[CH(SiMe₃)₂] with HC≡CPh; (b) thermolysis of (Cp*)₂Sm(C≡CPh)(THF) at 120–145 °C; (c) the reaction of [(Cp*)₂Sm(μ -H)]₂ with HC≡CPh; and (d) the reaction of (Cp*)₂Sm with HC≡CPh. This reactivity was also extended to include aliphatic terminal alkynes, HC≡CR (R = CH₂CH₂Ph, ^{*i*}Pent, and ^{*i*}Pr), leading to similar dinuclear trienediyl complexes [7]. However, when a more bulky acetylide is used (R = ^{*t*}Bu), the reaction halts at the formation of the alkynide monomers, e.g., the uncoupled dimer of the type [(Cp*)₂Sm(C≡C-^{*t*}Bu)]₂, which was prepared from the use of two different precursors; [(Cp*)₂Sm^{III}(μ -H)]₂, and (Cp*)₂Sm^{II}(THF) [7]. Alkyne dehydrocoupling has also been observed with copper salts [10] and titanium complexes [11].

Around the same period of time as the Evans report, two related contributions appeared in the literature. In particular, Teuben *et al.* [12] reported a study on early lanthanide carbyls, e.g., (Cp*)₂LnCH(SiMe₃)₂, that promote C–C coupling of terminal alkynes (HC≡CR) to give the corresponding trienediyl bimetallic species, {[(Cp*)₂Ln]₂(μ - η^2 : η^2 -RC₄R)} (Ln = Ce, R = Me or ^{*t*}Bu; Ln = La, R = Me). At the same time, Marks *et al.*, also reported the reaction of (Cp*)₂LaCH(SiMe₃) with HC≡CR (R = ^{*t*}Bu and Ph) to form the corresponding trienediyl dinuclear complexes [13]. The latter group concluded that the uncoupled dimer [(Cp*)₂La(C≡C–R)]₂ is the direct kinetic precursor of this reaction, and that neither a redox-active lanthanide ion nor a phenyl substituent on the alkyne is required for its completion. In a recent report from our group, we were able to shed light onto this type of reactivity by means of computational techniques [14]. Nevertheless, up until now, there has not been a clear picture of the alkyne coupling mechanism leading to dinuclear Sm(III) trienediyl complexes starting from low-valent samarocene (Figure 1).

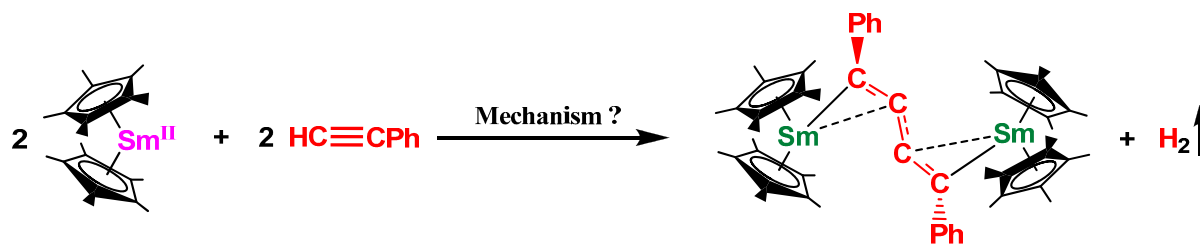


Figure 1. Reaction of samarocene with phenylacetylene to afford $\{[(C_5Me_5)_2Sm]_2(\mu-\eta^2:\eta^2-PhC_4-Ph)\}$ complex and H_2 .

The bimetallic mechanism which was previously proposed in the case of *N*-anchored tris(aryloxide) uranium(III) can serve as a base [15], but how acetylenic C–H bonds break to release H_2 still needs to be answered. Hence, in this paper we attempt to understand the performance of samarocene in the formation of the trinuclear complex, $\{[(Cp^*)_2Sm]_2(\mu-\eta^2:\eta^2-PhC_4-Ph)\}$, with plausible energetic reaction profiles being computed and suggested at the DFT (B3PW91) level of theory. The formation of the uncoupled complexes, instead of the trinuclear one where $tBuC\equiv CH$ was used, is also discussed. Based on these studies, novel transition states which lead to unique reaction pathways in the domain of *f*-block chemistry are revealed.

2. Results and Discussion

2.1. Dehydrocoupling of $PhC\equiv CH$ Using Cp^*_2Sm

Based on chemical intuition and previous knowledge on related mechanisms [15], three different types of reaction sequence are envisioned for this particular reactivity (Figure 2).

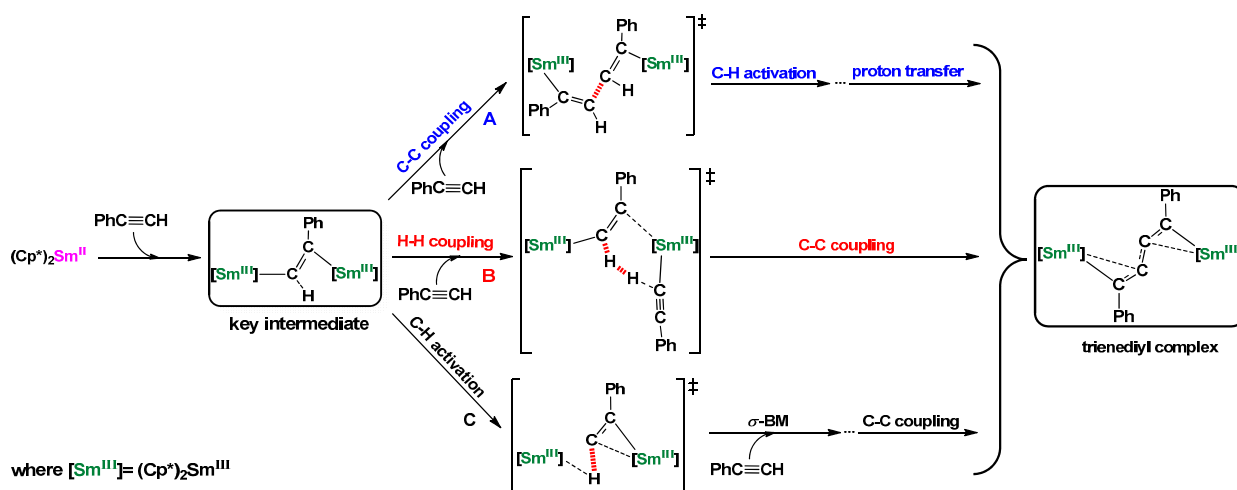


Figure 2. Possible reaction paths **A**, **B**, and **C** leading to the formation of the corresponding trinuclear complex using $PhC\equiv CH$ as the substrate and $(Cp^*)_2Sm$ as a precursor.

All these sequences share a common initiation step, the double SET one, in which a doubly reduced phenylacetylene unit contained in a dinuclear samarium(III) complex is formed. From this “key intermediate” the reaction can proceed either through: (A) a direct insertion of $PhC\equiv CH$ that leads to an alkynyl bis-Sm(III) complex; (B) a peculiar direct H–H coupling type of Transition State (TS);

(C) a C–H activation leading to a $\mu\text{-H}:\mu\text{-C}$ motif. Energetically the most favorable pathway relies on the C–H activation that corresponds to mechanism C and will be discussed in detail afterwards, together with the other routes. The whole energy profile for mechanism C is depicted in Figure 3.

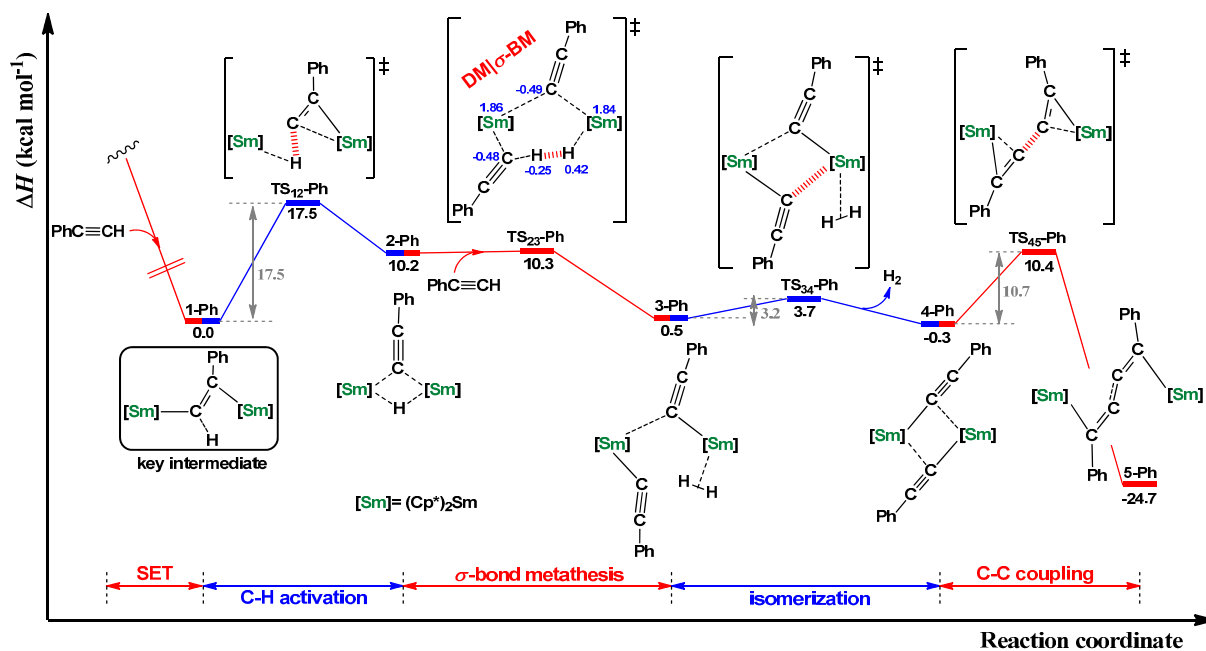


Figure 3. Enthalpy energy ΔH ($\text{kcal}\cdot\text{mol}^{-1}$) profile for the formation of the corresponding trienediyl complex using $\text{PhC}\equiv\text{CH}$ as substrate and $(\text{Cp}^*)_2\text{Sm}$ as a precursor (mechanism C). Cp^* ligands are omitted for clarity. Numbers in blue correspond to natural charges.

As already reported by us in a recent theoretical work, the one electron reduction of phenylacetylene, induced by the coordination to the samarium center, is a highly exothermic process [16]. This is the outcome of high level *ab-initio* calculations (CAS-SCF), but it is also based on the newly introduced theoretical methodology that takes into account the “HOMO-LUMO gap” energy difference. As the overall redox process is known to be exothermic, it contributes to the total energy stabilization of the newly formed “key intermediate” [17]. Hence, the latter species will be the reference point for the whole mechanism. In the **1-Ph** intermediate, the α - and β -carbons of the alkylenic substrate bind to each distinct Sm center in an *E*-configuration, with the *Z*-isomer being less stable by $3.6 \text{ kcal}\cdot\text{mol}^{-1}$ in accordance with earlier structural interpretation [18]. Interestingly, in **1-Ph**, the C–C bond distance of the sandwiched alkyne is 1.36 \AA which is 0.15 \AA longer than in free phenylacetylene. This is a strong indication of the double reduction of the alkyne. In addition, the acetylenic C–H bond points towards one Sm center and is elongated by 0.06 \AA with respect to free phenylacetylene, being readily available for a potential bond scission. At that point, the subsequent C–H bond activation (**TS12-Ph**) yielding a μ -hydride- μ -alkynyl dinuclear complex (**2-Ph**) can take place with a moderate energy barrier of $17.5 \text{ kcal}\cdot\text{mol}^{-1}$ with respect to the “key intermediate”. Hoffmann *et al.*, showed in a seminal work that extra stabilization is achieved by the mixing of the $1s$ orbital of the hydride with the available empty d_{z^2} and d_{yz} orbitals, of $1a_1$ and $1b_2$ symmetry respectively, of each $\text{Sm}(\text{Cp}^*)_2$ fragment [19]. This can nicely explain the relative low energy barrier computed for this step. It is noteworthy that this bridged dimer shares features with geometrically close

related yttrium complexes that were previously reported [20,21]. The reaction proceeds via **TS_{23-Ph}** that corresponds to the activation of the acetylenic proton of a second PhC≡CH molecule by the bridging hydride of complex **2-Ph**. This step is better described as a six-member σ -bond metathesis showing a negligible activation energy barrier. The alternation of the natural charge signs between the six atoms in **TS_{23-Ph}** (See Figure 3) and the respective shortening and lengthening of the bonds involved, confirms its σ -bond metathesis character. This is in line with previous studies [22–24]. To the best of our knowledge, this Dual Metal σ -Bond Metathesis transition state (DM| σ -BM) is the first report of such a type that implies two lanthanide centers working in concert. This type of transition state can be also found in other related lanthanide types of reactivity [25]. The latter step affords a μ -alkynyl- η^1 -alkynyl dihydrogen complex (**3-Ph**) that is almost isoenergetic with the “key intermediate”. In the subsequent step an isomerization takes place which induces the release of H₂, and leads to the formation of bis- μ -phenylacetylenyl complex, **4-Ph**. The formation of the latter requires a very low activation barrier ($\Delta_r H^\ddagger = 3.2 \text{ kcal}\cdot\text{mol}^{-1}$). From **4-Ph**, the final trienediyl dinuclear complex **5-Ph** is obtained by the C–C homocoupling of the two terminal μ -alkynyl moieties via **TS_{45-Ph}**. Interestingly, similar transition states were postulated to proceed in analogous systems, as for instance the bis- μ -alkynyl titanocene complexes [26]. In addition, analogous structures were structurally isolated and characterized for other lanthanide centers [12,27–29]. As already reported from our group, the energy barrier for the C–C coupling step is surprisingly low, being only $10.7 \text{ kcal}\cdot\text{mol}^{-1}$ [14]. This is odd since two negatively charged moieties have to be homocoupled. One way to accomplish this is to reduce the electron density of the negatively charged α -carbons of the alkynyls. This is achieved by the nucleophilic assistance from the β -carbon of each triple bond which accumulates enough negative charge, resulting in a stronger interaction with the second samarium center. Finally, the rate determining step of the entire mechanism is the scission of the C–H acetylenic bond ($17.5 \text{ kcal}\cdot\text{mol}^{-1}$), with the overall exothermicity of the mechanism being $24.7 \text{ kcal}\cdot\text{mol}^{-1}$ with respect to **1-Ph** intermediate.

The other two pathways depicted in Figure 1 were considered starting from **1-Ph**. In the first case (mechanism A), and inspired by our recent mechanistic work [15], the possibility of a direct C–C coupling in 1,1-fashion was investigated. This led to the corresponding Sm(III) bis-vinyl complex **6-Ph** (Figure 4). Although this step is strongly exothermic ($-31.0 \text{ kcal}\cdot\text{mol}^{-1}$), the activation barrier ($\Delta_r H^\ddagger = 24.8 \text{ kcal}\cdot\text{mol}^{-1}$) is much higher than the highest barrier of mechanism C, by more than $7 \text{ kcal}\cdot\text{mol}^{-1}$. The reaction involves an ionic transition state, **TS_{16-Ph}**, in which the incoming triple bond is polarized by one samarium center, allowing the formation of a lone-pair at the β -carbon atom and an empty sp^2 -orbital at its α -carbon that overlaps with the filled sp^2 -orbital of the α -carbon of the bridged reduced triple bond. This transition state closely resembles the one reported for the C–C coupling of the hex-1-yne using *N*-anchored tris-aryloxy complexes of U(III) [15]. Then the reaction proceeds through the activation of the C–H bond in close vicinity to the Sm center, surmounting an even higher activation barrier than the previous step ($\Delta_r H^\ddagger = 25.7 \text{ kcal}\cdot\text{mol}^{-1}$). The geometry of the intermediate that results, **7-Ph**, corresponds to a weakly coordinated complex, in which two fragments develop an H–H interaction (Figure 4). The latter undergoes a proton transfer to give the trienediyl compound upon release of H₂, via a transition state of relatively low activation barrier ($\Delta_r H^\ddagger = 6.9 \text{ kcal}\cdot\text{mol}^{-1}$). However, this mechanism can be ruled out from further consideration since it suffers kinetically from two relatively high activation barriers of *ca.* $24 \text{ kcal}\cdot\text{mol}^{-1}$, and thermodynamically by the formation of the highly stable bis-vinyl complex **6-Ph**. The latter

corresponds to the lowest energy point of the mechanism, being $6.3 \text{ kcal}\cdot\text{mol}^{-1}$ lower than the final trienediyl complex, as depicted in Figure 4.

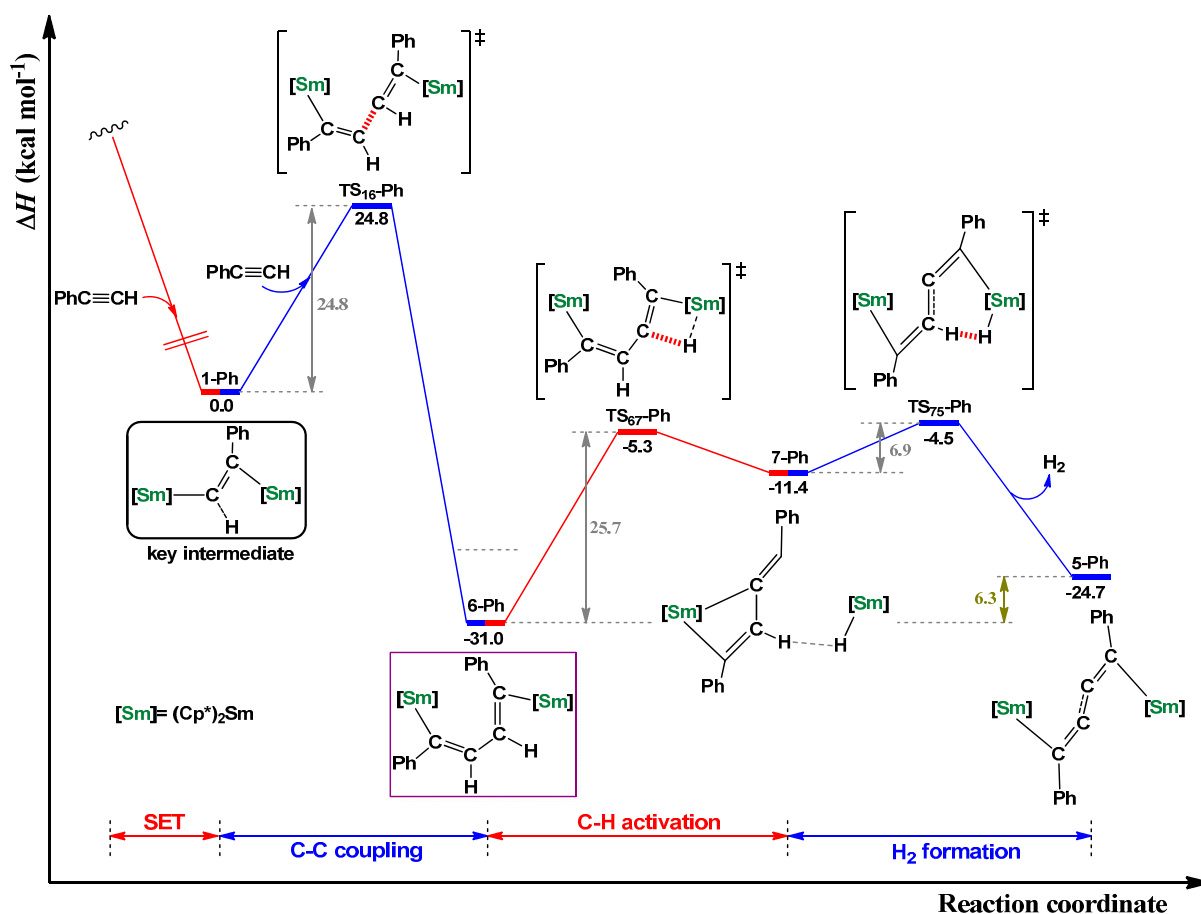


Figure 4. Enthalpy energy ΔH ($\text{kcal}\cdot\text{mol}^{-1}$) profile for the formation of the corresponding trienediyl complex using $\text{PhC}\equiv\text{CH}$ as substrate and $(\text{Cp}^*)_2\text{Sm}$ as a precursor (mechanism A). Cp^* ligands are omitted for clarity.

Finally, from “key intermediate” **1-Ph**, a mechanism that eliminates H_2 and homocouples the two alkynyls in a concerted homolytic manner (mechanism B) was attempted. Despite our efforts, we were unable to locate any transition state of this type. Instead, we found the direct formation of H_2 , but without any C–C coupling, leading to **5-Ph** after reorganization (Figure 5, mechanism B). By examining the nature of each hydrogen at the transition state, this can be regarded as an H–H coupling type of TS. Interestingly, the corresponding natural charges of the two hydrogens are -0.01 and $0.10 |e|$ (Figure 5). The first charge corresponds to the acetylenic bridged hydrogen, while the second belongs to the newly inserted alkyne. Nevertheless, the activation energy barrier for this step ($\Delta_r H^\ddagger = 27.2 \text{ kcal}\cdot\text{mol}^{-1}$) allows us to discard this pathway from further consideration.

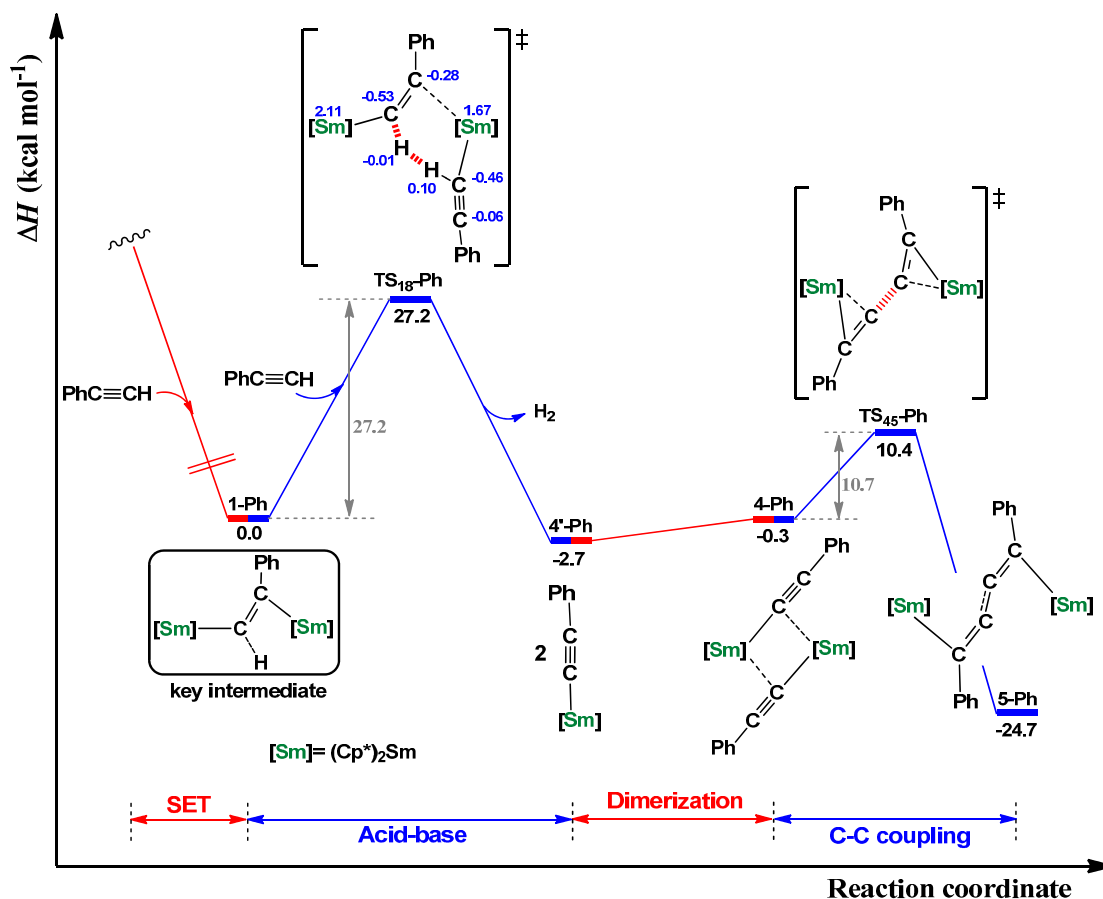


Figure 5. Enthalpy energy ΔH ($\text{kcal}\cdot\text{mol}^{-1}$) profile for the formation of the corresponding trienediyl complex using $\text{PhC}\equiv\text{CH}$ as substrate and $(\text{Cp}^*)_2\text{Sm}$ as a precursor (Mechanism B). Cp^* ligands are omitted for clarity. Numbers in blue correspond to natural charges.

In contrast, when a monometallic mechanism is operating, the C–C coupling can occur in 1,1 or 1,2 fashion (Figure S1 in supplementary information). In particular, addition of a second alkyne molecule to the $(\text{Cp}^*)_2\text{Sm}^{\text{III}}(\text{HC}\equiv\text{CPh})$ intermediate can take place in two different ways; in 1,1 and 1,2 fashion, affording the corresponding bis-vinyl species. The activation barriers were found to be 9.8 and 5.9 $\text{kcal}\cdot\text{mol}^{-1}$ respectively, with the exothermicities of each one being 31.1 and 27.7 $\text{kcal}\cdot\text{mol}^{-1}$ with respect to the monoreduced intermediate, $(\text{C}_5\text{Me}_5)_2\text{Sm}(\text{HC}\equiv\text{CPh})$. The computed small energy difference between the two transition states, as well as the preference for 1,2 C–C coupling, cannot account for the observed experimental selectivity which is found to be the reverse. On top of that, another weak point of the monometallic mechanism is the fact that after the formation of bis-vinyl monomeric complex, an oxidation of a second $\text{Sm}^{\text{II}}(\text{Cp}^*)_2$ has to take place. This will result in the formation of the same energetically buried bis-vinyl intermediate, **6-Ph**, as described previously in mechanism A. Since the formation of the latter is undesired, for the reasons described above, the existence of a monometallic pathway can also be ruled out.

2.2. Dehydrocoupling of $t\text{BuC}\equiv\text{CH}$ Using Cp^*Sm

We then turned our attention to include the more bulky $\text{H}-\text{C}\equiv\text{C}-t\text{Bu}$ alkyne that is found to give monomeric acetylide complexes rather than bimetallic trienediyl complexes [7], with the mechanism C applied to the new alkyne (Figure 6).

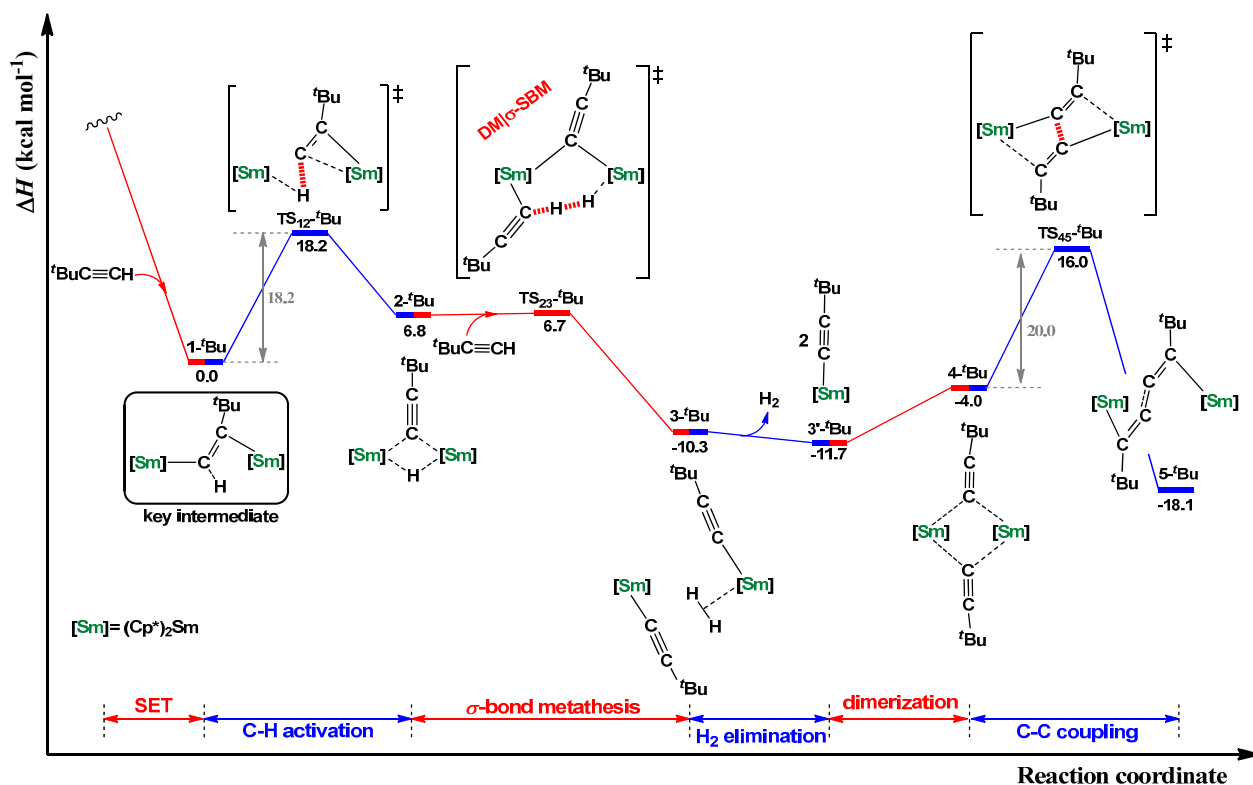


Figure 6. Enthalpy energy ΔH ($\text{kcal}\cdot\text{mol}^{-1}$) profile for the formation of the uncoupled alkynide complex using $t\text{BuC}\equiv\text{CH}$ as substrate and $(\text{Cp}^*)_2\text{Sm}$ as a precursor. Cp^* ligands are omitted for clarity.

Unlike the previous case, the first step corresponds to SET but with a concomitant dissociation of a THF molecule; the latter molecule being coordinated to the precursor complex $\text{Sm}(\text{Cp}^*)_2$. It is expected that the high energy gain observed in this step will be sufficient for the easy dissociation of the THF molecule. The latter is computed to cost around $10 \text{ kcal}\cdot\text{mol}^{-1}$ as it is depicted in Figure 7a. In addition, the isodesmic reaction of the net exchange of THF with the *t*-butylacetylene costs only $7.3 \text{ kcal}\cdot\text{mol}^{-1}$, indicative of the low amount of energy needed for such a reaction (Figure 7b). It should be noted that all the attempts to locate a local minimum that corresponds to the “key intermediate” with at least one THF coordinated to a samarium center were not successful, due to steric reasons. Hence, most likely the THF dissociates to yield the more energetically stable bimetallic intermediate $1-t\text{Bu}$.

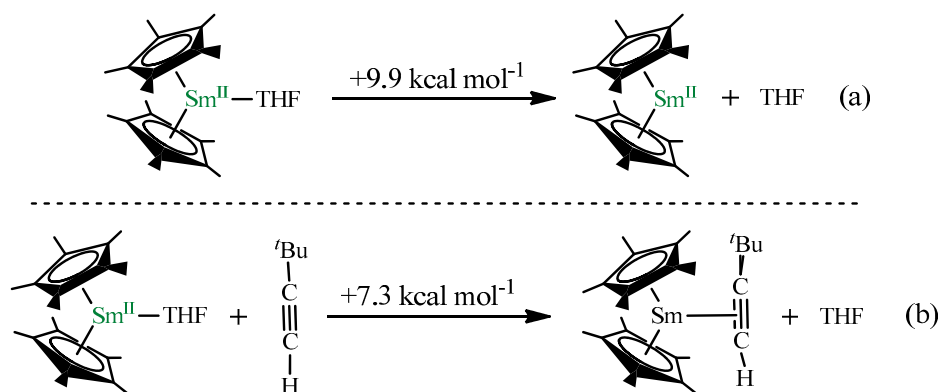


Figure 7. (a) Dissociation reaction of THF from the mono-solvated samarocene complex; (b) Exchange reaction of mono-solvated (THF) samarocene complex with $t\text{BuC}\equiv\text{CH}$.

Therefore, as in the phenylacetylene case, the “key intermediate” **1- $t\text{Bu}$** is considered as the starting point of the whole enthalpy profile. It is noteworthy that the first two steps are found to possess similar energy variations with that of phenylacetylene. This was not expected initially since the bulkier $t\text{BuC}\equiv\text{CH}$ will introduce more steric repulsions when it is sandwiched between the two samarocene moieties. This was especially anticipated in the C–H activation step, being in very close proximity to the two pentamethylcyclopentadienyl groups. Nevertheless, the inherent flexibility of the system probably allows the minimization of such repulsive forces by directing the methyl groups of the $t\text{Bu}$ to lie in an optimal position among the four Cp^* ligands. The only, but major differentiation with respect to the phenylacetylene case is the geometry of the product of the $\text{DM}|\sigma\text{-BM}$ step. The outcome of this process, computationally, is the disruption of the bimetallic complex into two monomeric alkynyl complexes, with one bearing a weakly coordinated dihydrogen molecule. Hence, instead of the generation of a $\mu\text{-alkynyl-}\eta^1\text{-alkynyl}$ dihydrogen-like complex, as is found in the $\text{PhC}\equiv\text{CH}$ case, e.g., **3-Ph**, the formation of the two monomers leads to a substantial energy stabilization (being $10.3\text{ kcal}\cdot\text{mol}^{-1}$ lower than the reference point). Then the system releases H_2 very easily to gain an extra energy stabilization of $1.4\text{ kcal}\cdot\text{mol}^{-1}$ and to yield consequently the well separated alkynyl complexes **3- $t\text{Bu}$** . The latter were experimentally observed as the only product of such reactivity [7]. Following this, the reaction can potentially proceed into the subsequent C–C coupling requiring a considerable amount of energy ($\Delta_r H^\ddagger = 27.7\text{ kcal}\cdot\text{mol}^{-1}$), kinetically hardly accessible [14]. Overall, the formation of the separated alkynyl species corresponds to the lowest point of the whole reaction route, being in perfect agreement with the experimental observations.

2.3. Dehydrocoupling of Hex-1-yne Using Cp^*_2Sm

To understand the effect induced by an alkyl substituent on the alkyne, we considered computationally the aliphatic hex-1-yne in order to check how this differentiates from the bulky $t\text{BuC}\equiv\text{CH}$, and the $\text{PhC}\equiv\text{CH}$ in which there is an extended conjugation of the triple bond with the phenyl ring. Even though the gain in energy is large for the double reduction of the hex-1-yne, as it was computed in a previous work by our group [16], it is half of that obtained for the phenylacetylene, possibly due to the delocalization of the extra electron(s) into the phenyl ring. In Figure 8, the most favorable reaction pathway is presented, reverting again to mechanism C.

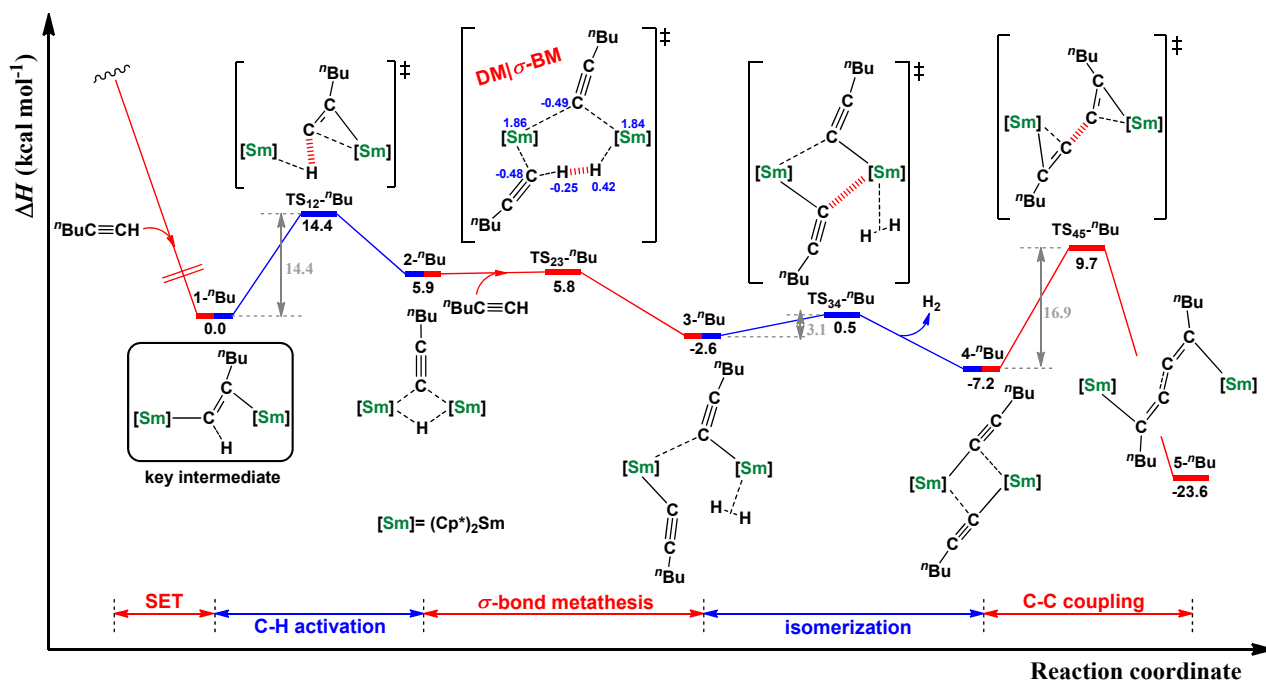


Figure 8. Enthalpy energy ΔH ($\text{kcal}\cdot\text{mol}^{-1}$) profile for the formation of the trienediyl complex using ${}^n\text{BuC}\equiv\text{CH}$ as substrate and $(\text{Cp}^*)_2\text{Sm}$ as a precursor. Cp^* ligands are omitted for clarity. Numbers in blue correspond to natural charges.

The geometry of the “key intermediate”, **1- ${}^n\text{Bu}$** , is similar to that found in the two previously described cases with the α - and β -carbons of the doubly reduced triple bond adopting a zig-zag geometry. In the same way, the acetylenic C–H bond is elongated by 0.08 Å (with respect to the free hex-1-yne) being already prepared for the forthcoming intramolecular C–H bond scission. Next, the aforementioned C–H bond activation takes place yielding a μ -hydride- μ -alkynyl dinuclear intermediate with an enthalpy activation barrier of 14.4 $\text{kcal}\cdot\text{mol}^{-1}$. This activation barrier is lower than the two previous by almost 4 $\text{kcal}\cdot\text{mol}^{-1}$. This is probably attributed to the reduced steric hindrance that substituents as ${}^n\text{Bu}$ -, and Ph- to a smaller extent, are inducing compared to the ${}^t\text{Bu}$ - one. The reaction can further proceed with the addition of a second hex-1-yne equivalent to form the bis- μ -alkynyl complex, **4- ${}^n\text{Bu}$** , after release of H_2 . This is achieved by passing through the **TS_{23- ${}^n\text{Bu}$}** , which corresponds to a barrierless process. The last step corresponds to the homo C–C coupling of the two μ -alkynyl moieties to afford the final trienediyl dinuclear complex. The activation barrier of this step ($\Delta_r H^\ddagger = 16.9 \text{ kcal}\cdot\text{mol}^{-1}$), is the highest of the entire mechanism, being consequently the rate determining step, contrary to the previous cases. Finally, this process is exothermic by 16.4 $\text{kcal}\cdot\text{mol}^{-1}$, while the overall reaction exothermicity is found to be 23.6 $\text{kcal}\cdot\text{mol}^{-1}$. Therefore, we conclude that the tested alkyne can be possibly used experimentally to afford, upon reaction with the Cp^*_2Sm complex, the corresponding trienediyl species. Concluding, apart from some small stabilization observed at the C–H bond activation transition state and the formation of the uncoupled dimeric species, **4- ${}^n\text{Bu}$** , with respect to the other two cases, the ${}^n\text{Bu}$ - substituent does not play any decisive role in the feasibility of such reactivity.

2.4. Dehydrocoupling of Various Terminal Alkynes Using $[\text{Cp}^*_2\text{Sm}(\mu\text{-H})_2]_2$ Complex

As described in the introduction, two experiments were conducted by Evans *et al.*, for the formation of the potential trienediyl complexes using ${}^t\text{BuC}\equiv\text{CH}$. The first was already investigated in detail in Section 2.2. In the second experiment, the bis-hydride dimer of Sm(III) was used, but as in the first case, it did not lead to the expected homocoupled product but instead to the formation of the uncoupled alkynide complexes as major product. It should also be noted that when $\text{PhC}\equiv\text{CH}$ is considered using the same precursor, $[\text{Cp}^*_2\text{Sm}(\mu\text{-H})_2]_2$, it yields the corresponding trienediyl complex. Therefore, a mechanistic investigation at the B3PW91 level of theory was carried out in order to discover the reason for this experimentally observed discrepancy and to propose a rational mechanism. As a reasonable mechanistic scenario we envisioned two consecutive (DM| σ -BM– H_2 release) steps (Figure 9a). Interestingly, for the phenylacetylene case, the first DM| σ -BM type of transition state surmounts a relative low activation barrier ($\Delta_r H^\ddagger = 10.5 \text{ kcal}\cdot\text{mol}^{-1}$). The intermediate **2-Ph** formed after the H_2 release (the isomerization step) is energetically stable enough, being $7.9 \text{ kcal}\cdot\text{mol}^{-1}$ lower than the starting material. The following part of the mechanism is essentially the same as proposed in mechanism C and consequently will not be discussed further. Finally, it is worth noting that a potential equilibrium between the dimer **9** and its mono-hydride structure was found computationally in favor of the dimer by $16.5 \text{ kcal}\cdot\text{mol}^{-1}$ in terms of enthalpy energy, in direct agreement with the experimentally observed thermal stability of **9** [18]. Hence, any mechanistic scenario starting from the monomeric complex was not considered in our studies.

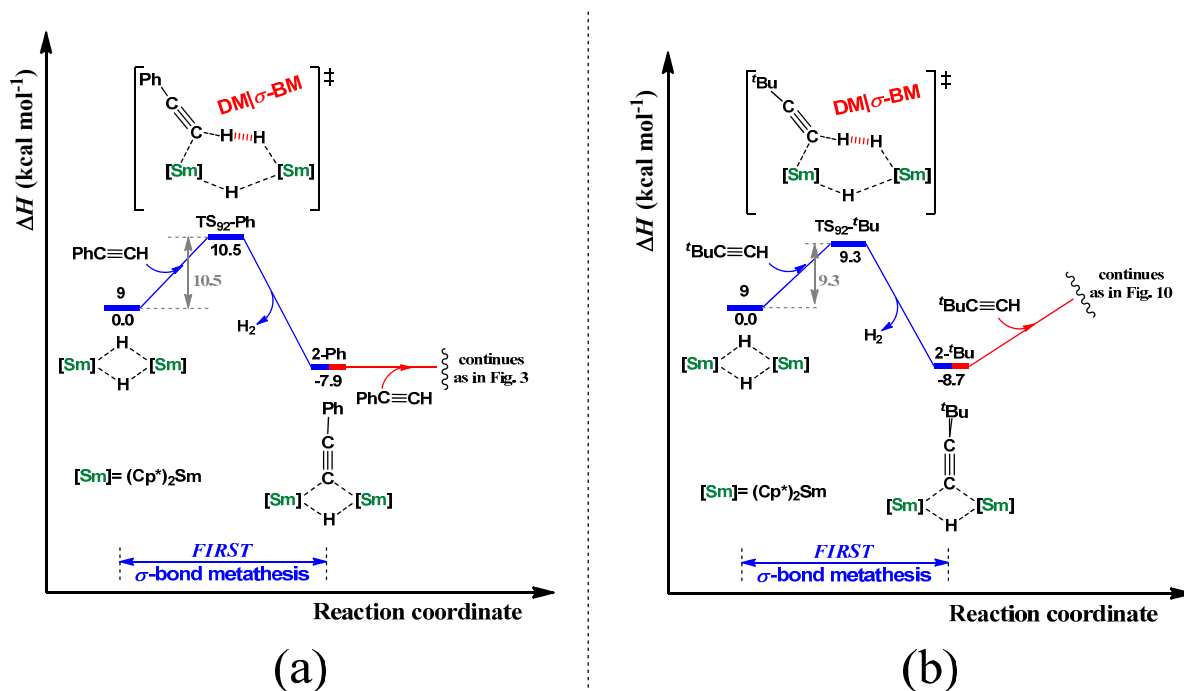


Figure 9. Enthalpy energy ΔH ($\text{kcal}\cdot\text{mol}^{-1}$) profiles for the formation of the corresponding trienediyl complexes using (a) $\text{PhC}\equiv\text{CH}$, and (b) ${}^t\text{BuC}\equiv\text{CH}$ as substrates, and $[(\text{Cp}^*)_2\text{Sm}(\mu\text{-H})_2]_2$ as a precursor. Cp^* ligands are omitted for clarity.

The same energy reaction pattern was considered in the case of $t\text{BuC}\equiv\text{CH}$. Again, the first step corresponds to a low energy process, even lower than for the phenylacetylene, with sufficient energy stabilization upon H_2 release, being almost isoenergetic to that obtained for $\text{PhC}\equiv\text{CH}$. However, unlike $\text{PhC}\equiv\text{CH}$, the second $\text{DM}|\sigma\text{-BM}$ step yields the uncoupled alkynyl complex, as was the case in the divalent samarocene, from which the C–C coupling is not kinetically easily accessible (Figure 9b). Hence, such type of two consecutive ($\text{DM}|\sigma\text{-BM}\text{-H}_2$ release) steps can serve as an explanation of the experimentally observed reactivity, shedding ample light into this peculiar reactivity in lanthanide chemistry.

3. Computational Section

All the quantum calculations, required for the delineation of the intermediate and transition state molecular structures, were performed at the density functional theory level using the B3PW91 [30,31] hybrid functional as implemented in the Gaussian program code [32]. The basis set used for the samarium atoms was the Stuttgart–Dresden–Köln (large-core) [33], augmented by an f polarization function in conjunction with the appropriate scalar relativistic pseudopotential [34]. For all the remaining atoms the all-electron double zeta basis set 6–31 G (d,p) was used [35,36]. Enthalpy energies were obtained at $T = 298.15$ K based on the harmonic approximation. Intrinsic Reaction Paths (IRPs) were traced from the various transition structures to verify the reactant to product linkage [37,38]. Natural population analysis (NPA) was performed using Weinhold's methodology [39,40].

4. Conclusions

Although the reaction of a low-valent samarocene with terminal alkynes affording a trienediyl binuclear complex and H_2 seems simple, the mechanism underlying this transformation is mechanistically complicated. In the present DFT mechanistic study, the cooperativity of the two lanthanides is highlighted, with a unique mechanistic scenario being proposed, involving novel type of transition states, such as the $\text{DM}|\sigma\text{-SBM}$, for example. In this particular saddle point of the potential energy surface, the two samarium centers are working synergistically to facilitate H_2 elimination, by forming a six-member transition state. It is worth noting that this type of transition state consists of a novel paradigm of σ -bond metathesis that can be added to the already well-established related types [41]. Among other mechanistic paths, the operating mechanism consists of (i) the oxidation of each samarium center and the concomitant double reduction of the alkyne to afford a binuclear intermediate; (ii) the C–H scission of the acetylinic bond that lies in between the two metals; (iii) a $\text{DM}|\sigma\text{-SBM}$ process that releases the H_2 molecule; (iv) the C–C coupling of the two bridged μ -alkynides to give the final experimentally observed bimetallic trienediyl complex. For the latter mechanistic route the experimentally used substrate, phenylacetylene, was considered first, and afterwards the hex-1-yne in order to check the effect of the alkyl substituent. For the aliphatic alkyne, the applied mechanism leads to the same conclusions in terms of enthalpy of reaction, making this process feasible experimentally. On the other hand, the lack of obtaining the trienediyl analogs when the $t\text{BuC}\equiv\text{CH}$ is used, as reported experimentally, is due to the thermodynamic preference for disruption of the bimetallic product of the $\text{DM}|\sigma\text{-SBM}$ step over the homocoupling of the two bulky alkynyl moieties. We strongly believe that this computational contribution sheds light into the

mechanism at work in this peculiar reactivity, and will help in the direction of additional understanding in the future of organolanthanide chemistry.

Supplementary Materials

Supplementary materials can be found at <http://www.mdpi.com/2304-6740/3/4/0573/s1>.

Acknowledgments

Laurent Maron is member of the Institute Universitaire de France. CINES (Centre Informatique National de l'Enseignement Supérieur) and CALMIP (Calcul en Midi-Pyrénées) are acknowledged for a generous grant of computing time. The Humboldt Foundation and The Chinese Academy of Science are also acknowledged. The authors are grateful to Lionel Perrin for fruitful discussions and comments on various aspects of the present work.

Author Contributions

Laurent Maron conceived the project; Christos E. Kefalidis performed the calculations; Laurent Maron and Christos E. Kefalidis analyzed the data and wrote the manuscript.

Conflicts of Interest

The authors declare no conflict of interest.

References

1. Krief, A.; Laval, A.-C. Coupling of organic halides with carbonyl compounds promoted by SmI₂, the Kagan reagent. *Chem. Rev.* **1999**, *99*, 745–777.
2. Procter, D.J.; Flowers, R.A., II; Skrydstrup, T. *Organic Synthesis Using Samarium Diodide: A Practical Guide*; Royal Society of Chemistry Publishing: Cambridge, UK, 2010.
3. Evans, W.J.; Chamberlain, L.R.; Ulibarri, T.A.; Ziller, J.W. Reactivity of trimethylaluminum with (C₅Me₅)₂Sm(THF)₂: Synthesis, structure, and reactivity of the samarium methyl complexes (C₅Me₅)₂Sm[(μ-Me)AlMe₂(μ-Me)]₂Sm(C₅Me₅)₂ and (C₅Me₅)₂SmMe(THF). *J. Am. Chem. Soc.* **1988**, *110*, 6423–6432.
4. Nolan, S.P.; Stern, C.L.; Marks, T.J. Organo-*f*-element thermochemistry. Absolute metal-ligand bond disruption enthalpies in bis(pentamethylcyclopentadienyl)samarium hydrocarbyl, hydride, dialkylamide, alkoxide, halide, thiolate, and phosphide complexes. Implications for organolanthanide bonding and reactivity. *J. Am. Chem. Soc.* **1989**, *111*, 7844–7853.
5. Evans, W.J.; Ulibarri, T.A.; Ziller, J.W. Reactivity of (C₅Me₅)₂Sm with aryl-substituted alkenes: Synthesis and structure of a bimetallic styrene complex that contains an η²-arene lanthanide interaction. *J. Am. Chem. Soc.* **1990**, *112*, 219–223.
6. Evans, W.J.; Ulibarri, T.A.; Ziller, J.W. Reactivity of (C₅Me₅)₂Sm and related species with alkenes: Synthesis and structural characterization of a series of organosamarium allyl complexes. *J. Am. Chem. Soc.* **1990**, *112*, 2314–2324.

7. Evans, W.J.; Keyer, R.A.; Ziller, J.W. Investigation of organolanthanide-based carbon–carbon bond formation: Synthesis, structure, and coupling reactivity of organolanthanide alkynide complexes, including the unusual structures of the trienediyl complex $[(C_5Me_5)_2Sm]_2[\mu-\eta^2:\eta^2-Ph(CH_2)_2C=C=C-(CH_2)_2Ph]$ and the unsolvated alkynide $[(C_5Me_5)_2Sm(C\equiv CMe_3)]_2$. *Organometallics* **1993**, *12*, 2618–2633.
8. Evans, W.J.; Davis, B.L. Chemistry of tris(pentamethylcyclopentadienyl) *f*-element complexes, $(C_5Me_5)_3M$. *Chem. Rev.* **2002**, *102*, 2119–2136.
9. Evans, W.J.; Keyer, R.A.; Ziller, J.W. Carbon–carbon bond formation by coupling of two phenylethynyl ligands in an organolanthanide system. *Organometallics* **1990**, *9*, 2628–2631.
10. Wood, G.L.; Knobler, C.B.; Hawthorne, M.F. Synthesis of $Cp_2Ti[C\equiv CSi(CH_3)_3]_2$ and the synthesis and molecular structure of $[Cp_2TiC\equiv CSi(CH_3)_3]_2$. *Inorg. Chem.* **1989**, *28*, 382–384.
11. Sekutowski, D.G.; Stucky, G.D. Oxidative coupling of the phenylethynyl group in μ -(1-3 η :2-4 η -*trans,trans*-1,4-diphenylbutadiene)-bis(bis(η^5 -methylcyclopentadienyl)titanium) and the reaction of 1,4-diphenyl-1,3-butadiene with bis(cyclopentadienyl)titanium(II). *J. Am. Chem. Soc.* **1976**, *98*, 1376–1382.
12. Heeres, H.J.; Nijhoff, J.; Teuben, J.H. Reversible carbon–carbon bond formation in organolanthanide systems. Preparation and properties of lanthanide acetylides $[Cp^*_2LnC\equiv CR]_n$ and their rearrangement products $[Cp^*_2Ln]_2-\mu-\eta^2:\eta^2-RC_4R$ ($Ln = La, Ce$; $R = \text{alkyl}$). *Organometallics* **1993**, *12*, 2609–2617.
13. Forsyth, C.M.; Nolan, S.P.; Stern, C.L.; Marks, T.J.; Rheingold, A.L. Alkyne coupling reactions mediated by organolanthanides. Probing the mechanism by metal and alkyne variation. *Organometallics* **1993**, *12*, 3618–3623.
14. Kefalidis, C.E.; Perrin, L.; Maron, L. Computational insights into carbon–carbon homocoupling reactions mediated by organolanthanide(III) complexes. *Dalton Trans.* **2014**, *43*, 4520–4529.
15. Kosog, B.; Kefalidis, C.E.; Heinemann, F.W.; Maron, L.; Meyer, K. Uranium(III)-mediated C–C-coupling of terminal alkynes: Formation of dinuclear uranium(IV) vinyl complexes. *J. Am. Chem. Soc.* **2012**, *134*, 12792–12797.
16. Kefalidis, C.E.; Essafi, S.; Perrin, L.; Maron, L. Qualitative estimation of the single-electron transfer step energetics mediated by samarium(II) complexes: A “SOMO–LUMO gap” approach. *Inorg. Chem.* **2014**, *53*, 3427–3433.
17. Labouille, S.; Nief, F.; Maron, L. Theoretical treatment of redox processes involving lanthanide(II) compounds: Reactivity of organosamarium(II) and organothulium(II) complexes with CO_2 and pyridine. *J. Phys. Chem. A* **2011**, *115*, 8295–8301.
18. Evans, W.J.; Bloom, I.; Hunter, W.E.; Atwood, J.L. Organolanthanide hydride chemistry. 3. Reactivity of low-valent samarium with unsaturated hydrocarbons leading to a structurally characterized samarium hydride complex. *J. Am. Chem. Soc.* **1983**, *105*, 1401–1403.
19. Ortiz, J.V.; Hoffmann, R. Hydride bridges between $LnCp_2$ centers. *Inorg. Chem.* **1985**, *24*, 2095–2104.
20. Schaverien, C.J. Alkoxides as ancillary ligands in organolanthanide chemistry: Synthesis of, reactivity of, and olefin polymerization by the μ -hydride- μ -alkyl compounds $[Y(C_5Me_5)(OC_6H_3^tBu_2)]_2(\mu-H)(\mu-alkyl)$. *Organometallics* **1994**, *13*, 69–82.

21. Duchateau, R.; van Wee, C.T.; Meetsma, A.; van Duijnen, P.T.; Teuben, J.H. Insertion and C–H bond activation of unsaturated substrates by bis(benzamidinato)yttrium alkyl, $[\text{PhC}(\text{NSiMe}_3)_2]_2\text{YR}$ ($\text{R} = \text{CH}_2\text{Ph}\cdot\text{THF}$, $\text{CH}(\text{SiMe}_3)_2$), and hydrido, $\{[\text{PhC}(\text{NSiMe}_3)_2]_2\text{Y}(\mu\text{-H})\}_2$, compounds. *Organometallics* **1996**, *15*, 2291–2302.
22. Steigerwald, M.L.; Goddard, W.A. The $2_s + 2_s$ reactions at transition metals. 1. The reactions of D_2 with Cl_2TiH^+ , Cl_2TiH , and Cl_2ScH . *J. Am. Chem. Soc.* **1984**, *106*, 308–311.
23. Ziegler, T.; Folga, E.; Berces, A. A density functional study on the activation of hydrogen–hydrogen and hydrogen–carbon bonds by $\text{Cp}_2\text{Sc-H}$ and $\text{Cp}_2\text{Sc-CH}_3$. *J. Am. Chem. Soc.* **1993**, *115*, 636–646.
24. Maron, L.; Eisenstein, O. DFT study of H–H activation by $\text{Cp}_2\text{LnH } d^0$ complexes. *J. Am. Chem. Soc.* **2001**, *123*, 1036–1039.
25. Ren, J.; Hu, J.; Lin, Y.; Xing, Y.; Shen, Q. The reactivity of lanthanide alkyl compounds with phenylacetylene: Synthesis and structure of $[(\text{Bu}'\text{Cp})_2\text{LnC}\equiv\text{CPh}]_2$ ($\text{Ln} = \text{Nd}, \text{Gd}$). *Polyhedron* **1996**, *15*, 2165–2169.
26. Cuenca, T.; Gómez, R.; Gómez-Sal, P.; Rodriguez, G.M.; Royo, P. Reactions of titanium- and zirconium(III) complexes with unsaturated organic systems. X-ray structure of $\{[(\eta^5\text{-C}_5\text{H}_5)\text{Zr}(\text{CH}_3)]_2[\mu\text{-}\eta^1\text{-}\eta^2\text{-CN}(\text{Me}_2\text{C}_6\text{H}_3)](\mu\text{-}\eta^5\text{-}\eta^5\text{-C}_{10}\text{H}_8)\}$. *Organometallics* **1992**, *11*, 1229–1234.
27. Atwood, J.L.; Hunter, W.E.; Evans, W.J. Synthesis and crystallographic characterization of a dimeric alkynide-bridged organolanthanide: $[(\text{C}_5\text{H}_5)_2\text{ErC}\equiv\text{CC}(\text{CH}_3)_3]_2$. *Inorg. Chem.* **1981**, *20*, 4115–4119.
28. Evans, W.J.; Bloom, I.; Hunter, W.E.; Atwood, J.L. Synthesis of organosamarium complexes containing Sm–C and Sm–P bonds. Crystallographic characterization of $[(\text{MeC}_5\text{H}_4)_2\text{SmC}\equiv\text{CCMe}_3]_2$. *Organometallics* **1983**, *2*, 709–714.
29. Shen, Q.; Zheng, D.; Lin, L.; Lin, Y. Synthesis of $(t\text{-C}_4\text{H}_9\text{C}_5\text{H}_4)_2\text{Sm}(\text{DME})$ and its reactivity with phenylacetylene: Synthesis and structure of $((t\text{-C}_4\text{H}_9\text{C}_5\text{H}_4)_2\text{SmC}\equiv\text{CPh})_2$. *J. Organomet. Chem.* **1990**, *391*, 307–312.
30. Becke, A.D. Density-functional thermochemistry. III. The role of exact exchange. *J. Chem. Phys.* **1993**, *98*, 5648–5652.
31. Perdew, J.P.; Wang, Y. Accurate and simple analytic representation of the electron-gas correlation energy. *Phys. Rev. B* **1992**, *45*, 13244–13249.
32. Gaussian 09, Revision A.02; Gaussian Inc.: Wallingford, CT, USA, 2009.
33. Dolg, M.; Stoll, H.; Savin, A.; Preuss, H. Energy-adjusted pseudopotentials for the rare earth elements. *Theor. Chim. Acta* **1989**, *75*, 173–194.
34. Dolg, M.; Stoll, H.; Preuss, H. A combination of quasirelativistic pseudopotential and ligand field calculations for lanthanoid compounds. *Theor. Chim. Acta* **1993**, *85*, 441–450.
35. Hehre, W.J.; Ditchfield, R.; Pople, J.A. Self-consistent molecular orbital methods. XII. Further extensions of Gaussian-type basis sets for use in molecular orbital studies of organic molecules. *J. Chem. Phys.* **1972**, *56*, 2257–2261.
36. Hariharan, P.C.; Pople, J.A. The influence of polarization functions on molecular orbital hydrogenation energies. *Theor. Chim. Acta* **1973**, *28*, 213–223.
37. Gonzalez, C.; Schlegel, H.B. An improved algorithm for reaction path following. *J. Chem. Phys.* **1989**, *90*, 2154–2161.

38. Gonzalez, C.; Schlegel, H.B. Reaction path following in mass-weighted internal coordinates. *J. Phys. Chem.* **1990**, *94*, 5523–5527.
39. Reed, A.E.; Curtiss, L.A.; Weinhold, F. Intermolecular interactions from a natural bond orbital, donor–acceptor viewpoint. *Chem. Rev.* **1988**, *88*, 899–926.
40. Weinhold, F. Natural bond orbital methods. In *Encyclopedia of Computational Chemistry*; Schleyer, P.V.R., Allinger, N.L., Clark, T., Eds.; John Wiley & Sons: Chichester, UK, 1998; Volume 3, pp. 1792–1811.
41. Waterman, R. σ -Bond metathesis: A 30-year retrospective. *Organometallics* **2013**, *32*, 7249–7263.

© 2015 by the authors; licensee MDPI, Basel, Switzerland. This article is an open access article distributed under the terms and conditions of the Creative Commons Attribution license (<http://creativecommons.org/licenses/by/4.0/>).